IEEE Access
Multidisciplinary | Rapid Review | Open Access Journal

Received April 21, 2019, accepted May 2, 2019, date of publication May 8, 2019, date of current version June 3, 2019.

Digital Object Identifier 10.1109/ACCESS.2019.2915509

Distributed Secondary Voltage Control of Islanded Microgrids Based on RBF-Neural-Network Sliding-Mode Technique

XUEQIANG SHEN, HAIQING WANG, JIAN LI, QINGYU SU, AND LAN GAO
School of Automation Engineering, Northeast Electric Power University, Jilin City 132012, China

Corresponding author: Qingyu Su (suqingyu@neepu.edu.cn)

This work was supported in part by the National Natural Science Foundation of China under Grant 61873057, Grant 61703384, and Grant 61703091, in part by the Natural Science Foundation of Jilin Province under Grant 20180520211JH and Grant 20190303107SF, and in part by the Jilin City Science and Technology Bureau under Grant 201831727 and Grant 201831731.

ABSTRACT The secondary voltage control problem of inverter-based islanded microgrid (MG) is proposed in this paper. First, the dynamics of the distributed generation (DG) with primary control is analyzed and modeled. Then, an RBF-neural-network (RBF-NN) sliding-mode controller is designed to eliminate the voltage deviation caused by primary control. The output voltage of all DGs can restore to a reference value and remains stable. Finally, taking an MG consisting of four DGs as an example, the experimental results validate the designed secondary control strategy.

INDEX TERMS Islanded microgrids, secondary voltage control, distributed, RBF-neural-network sliding-mode control.

I. INTRODUCTION

The dual pressures of environmental protection and energy depletion have forced us to develop clean renewable energy. In order to solve the large-scale grid connection problem of distributed generations (DGs), the concept of Microgrids (MG) is proposed [1]. MG is a small power distribution system consisting of distributed power sources, energy storage devices, energy conversion devices, loads, monitoring and protection devices. It is a system that can be controlled, protected and managed by itself. It not only can operate connecting the main grid in low and medium voltage, but also operate in islanded mode. Thus, MG is an effective way to realize the active distribution network, making the traditional grid transition to the smart grid.

Normally, the MG is connected to the main grid through a static switch. Since the capacity of the main grid is larger, the dynamics of the MG are dominated by the main grid [2], [3]. At this point, the control task of the MG is to transfer the planned active and reactive power to the main grid. Once the disturbance occurs, the static switch connected to the main grid of the MG will break, and the MG will be isolated. The MG control task is not only to make voltage stabile, but also reach a certain reference value. Therefore, the problem of islanded MG control has become the focus of research in the field of control [4].

Voltage stability of the power system can be considered as a problem of the complex system control with multiple voltage levels and control targets. Recently, the hierarchical control is the most mature and widely used MG control strategy with three layers generally [5], [6]. And the tertiary control is the highest layer, which optimizes the economic operation of the whole system and considers the stability index. The secondary control accepts the tertiary control signal to ensure that the voltage amplitude of the pilot node is approximately the preset value. If the voltage amplitude of the pilot node deviates, the secondary voltage controller will change the preset reference value of the primary voltage controller according to a predetermined control law. The primary voltage controller mainly comprising the automatic voltage regulator (AVR), on-load voltage regulator (OLTC) and static var compensator (SVC) for the local generator [7]. As the regional cooperative control, the secondary voltage control is the key to break through the local voltage control. It is the crucial link connecting the primary voltage control and the tertiary voltage control in the voltage hierarchical control system, and also the core of the hierarchical control research [8].

The associate editor coordinating the review of this manuscript and approving it for publication was Padmanabh Thakur.

The traditional secondary control depends on a central controller. It needs to collect all the information of each DG, and then send control commands to each DG. The communication network is complex and the communication volume is huge, which will reduce the stability of the system. In order to reduce the system's traffic and increase the stability of the system, in recent years, the distributed cooperative control strategy has been applied to the secondary control of the MG [9]. Each DG's controller communicates only with neighboring DGs. Thus, the central controller is not required. Which reduces system traffic and improves system robustness. Therefore, the distributed control strategy plays an important role in the area of MG control. More and more researchers study distributed control from different aspects. Considering that continuous-time methods may be inaccurate for this kind of dynamic study, due to discrete nature of the information exchange in the communication network, the author adopt a discrete-time approach in [10], [11]. There are some robust distributed control algorithms considering time-delay communications, limited communication bandwidth and uncertain communication links of communication network for distributed generation systems designed [12], [13]. In addition, the authors consider that simultaneous voltage regulation and reactive power sharing is not achieved, in presence of distribution line impedances. The voltage and reactive power control are discussed and studied respectively [14], [15]. These publications are comprehensive, meaningful and practical. The difference is that other excellent authors have studied the problem of MG control from another angle. For example, some control algorithms have been applied to the distributed cooperative control of each DG. In [16], the dynamics of the DG are analyzed, and the finite-time control algorithm is addressed to restore the DG voltage to the reference value. In [17], [18], the input-output feedback linearization method is applied to transform the secondary voltage control problem into a first-order synchronous tracking problem. In [19], the model predictive control (MPC) is used to solve problems such as load or communication changes in the MG. In [20], the author considers that the dynamics of DGs in the MG are nonlinear, and adopts the sliding mode variable structure control algorithm, a nonlinear algorithm. However, the issue of ''chatter reduction'' is not considered in the paper.

The main content of this paper includes the following points. 1) Considering the dynamics of each DG and the power network problem, a simplified model of the MG is established. 2) A distributed cooperative control strategy is adopted, and the RBF neural network combined with the sliding mode control is addressed. The sliding mode control can stabilize the system in a short time. In order to reduce the chattering phenomenon, RBF neural network is used to adjust switching gain of the sliding mode control in real time. The distributed RBF neural network sliding mode control is used to restore the MG voltage. 3) The desired response speed can be obtained by adjusting the controller parameters. The contributions of this paper is 2) and 3). The RBF-NN sliding-mode secondary controller is designed in this paper. The theory of this controller combines RBF neural network and sliding mode technique. In a word, the RBF-NN sliding-mode controller make the system stable timely, robust and solve the question of chattering reduction.

The remainder of this paper is as follows: In Section 2, we analyze the dynamics of the MG and build its model. The Section 3 is the design and analysis of the distributed secondary voltage controller. In Section 4, the simulation results are analyzed to verify the effectiveness of the secondary controller. The Section 5 summarizes the paper.

II. MODELING OF MG

A. INVERTER-BASED DG MODEL

Generally, hierarchical control strategy consists of primary, secondary and tertiary control, employed in MG control, where the primary control is local control of each DG. The output voltage of the MG can keep stable with the load or power generation of the system changes or when the MG is in islanded mode.

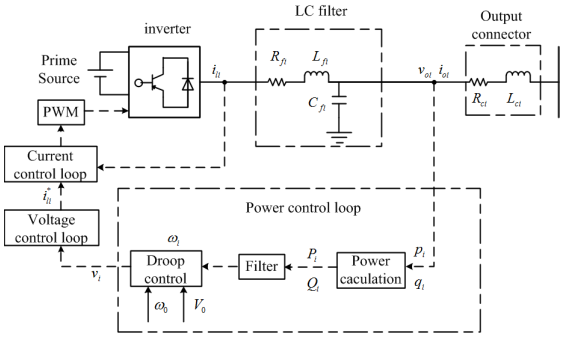

FIGURE 1. Primary control schematic diagram of an inverter-based DG.

The primary control schematic of DG is shown as Fig.1. In general, the voltage source inverter (VSI) based DG unit consists of a dc/ac inverter bridge, a prime dc source, an inductor-capacitor (LC) filter and a Resistor-inductor (RL) output connector. In addition, there exists voltage, current and power control loops. It can be known that the dynamics of voltage and current control loops are faster than the power control loop [21]. Therefore, in the primary control model, only the droop control function of power control loop is considered for simplification. The principle of primary and secondary control is showed as Fig.2. It is the procedure of voltage regulation based on droop control. The objective of primary control is to maintain the voltage magnitude near around its nominal values once user demands and/or power supply changes, while the secondary control is employed to restore the deviations produced by the primary control [9], [15]. As seen in Fig.2, the procedure from point A to B represents primary control, and from point B to C represents secondary control.

According to the droop control detailed in [22], the relationship equation between the output voltage and the reactive

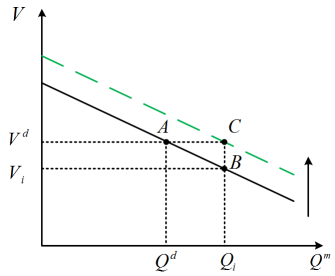

FIGURE 2. Procedure of voltage regulation.

power of the DG can be represented as:

$$V_i = V^d - n_{Q_i} Q_i^m \tag{1}$$

where V_i is the output voltage amplitude of ith DG, V^d is the desired voltage amplitude, n_{Q_i} is the droop coefficient of ith DG, Q_i^m is the measured reactive power locally.

The relationship between the measured reactive power Q_i^m and the reactive power Q_i of the filter output in the process is:

$$\tau_{Q_i} \dot{Q}_i^m = -Q_i^m + Q_i \tag{2}$$

According to [16], equations (1) and (2), a dynamics equation representing the primary control of the ith DG can be obtained:

$$\tau_{Q_i} k_{V_i} \ddot{V}_i + (\tau_{Q_i} + k_{V_i}) \dot{V}_i + V_i - V^d + k_{Q_i}(Q_i - Q_i^d) = 0 \tag{3}$$

B. NETWORK MODEL

According to the graph theory detailed in [10], [14], [23], we consider the communication network of MG system as a undirected graph to control output voltages of multiple DGs reach the preset value cooperatively. The ith node represents the ith DG (bus), and the line between the ith and the jth nodes represents the association between the two DGs, i.e., the admittance on the line $Y_{ij} = G_{ij} + jB_{ij}$. If for $j \notin N_i$, then $Y_{ij} = 0$. If for $j \notin N_i$, then $Y_{ij} = 0$. If $j \in N_i$, and $j \neq i$, then $Y_{ij} \neq 0$. The admittance matrix is similar to the Laplacian matrix, which characterizes the topology and line weight of the MG.

Assumption 1: The power transmission lines of the MG network are lossless, i.e., $G_{ij} = 0$, $Y_{ij} = jB_{ij}$, and $\phi_{ij} = \phi_{ji} = -(\pi/2)$, $\forall j \in N_i$.

Assumption 2: The local loads are connected to each DG.

The apparent power injected at the ith DG inverter is set as $S_{Ii} = P_{Ii} + jQ_{Ii}$. Where P_{Ii} and jQ_{Ii} are the active power and reactive power injected by the ith inverter into the MG, respectively [24].

$$Q_{Ii} = V_i^2 \sum_{j \in N_i} |B_{ij}| - \sum_{j \in N_i} |B_{ij}| V_i V_j \cos(\delta_i - \delta_j) \tag{4}$$

According to the power balance relationship in the power grid, the output power of the ith inverter is the sum of the power consumed by the local load and the power injected into the power grid [25], that is,

$$\begin{aligned} P_i &= P_{Li} + P_{Ii} \\ Q_i &= Q_{Li} + Q_{Ii} \end{aligned} \tag{5}$$

According to the ZIP load model [26], the local load power can be expressed as a quadratic polynomial of the local voltage amplitude V_i.

$$\begin{aligned} P_{Li} &= P_{1_i} V_i^2 + P_{2_i} V_i + P_{3_i} \\ Q_{Li} &= Q_{1_i} V_i^2 + Q_{2_i} V_i + Q_{3_i} \end{aligned} \tag{6}$$

Combining (4), (5) and (6), the output power expression is derived as:

$$\begin{aligned} Q_i = Q_{1_i} V_i^2 + Q_{2_i} V_i + Q_{3_i} + V_i^2 \sum_{j \in N_i} |B_{ij}| \\ - \sum_{j \in N_i} |B_{ij}| V_i V_j \cos(\delta_i - \delta_j) \end{aligned} \tag{7}$$

Introduce the secondary control variable u_i to the primary control model (3) and get the following formula:

$$\tau_{Q_i} k_{V_i} \ddot{V}_i + (\tau_{Q_i} + k_{V_i}) \dot{V}_i + V_i - V^d + k_{Q_i}(Q_i - Q_i^d) + u_i = 0 \tag{8}$$

Combining the models of DG and network, we can derive the MG model. We denote $x_i = [V_i \quad \dot{V}_i]$, and write the system in terms of a state space expression as:

$$\begin{cases} \dot{x}_i = \begin{bmatrix} 0 & 1 \\ 0 & 0 \end{bmatrix} x_i + \begin{bmatrix} 0 \\ f_i(x_i, x_j) \end{bmatrix} + \begin{bmatrix} 0 \\ g_i \end{bmatrix} u_i \\ y_i = \begin{bmatrix} 1 & 0 \end{bmatrix} x_i \end{cases} \tag{9}$$

where $g_i = \frac{1}{\tau_{Q_i} k_{V_i}}$, and $f_i(x_i, x_j)$ can be derived from eq.(3) and eq.(7):

$$\begin{aligned} f_i(x_i, x_j) = &- \frac{\tau_{Q_i} + k_{V_i}}{\tau_{Q_i} k_{V_i}} \dot{V}_i - \frac{k_{Q_i}(Q_{1_i} + \sum_{j \in N_i} |B_{ij}|)}{\tau_{Q_i} k_{V_i}} V_i^2 \\ &+ \frac{k_{Q_i}}{\tau_{Q_i} k_{V_i}} \sum_{j \in N_i} |B_{ij}| V_i V_j \cos(\delta_i - \delta_j) \\ &- \frac{1 + k_{Q_i} Q_{2_i}}{\tau_{Q_i} + k_{V_i}} V_i - \frac{k_{Q_i}(Q_{3_i} - Q_i^d - V^d)}{\tau_{Q_i} + k_{V_i}} \end{aligned} \tag{10}$$

A secondary controller for the MG system with hierarchical control strategy is designed in this paper, in order to compensate for the voltage deviation caused by the primary control. Finally, the output voltages of all distributed DGs are synchronized to the reference voltage V_r. The framework of the hierarchical control for a MG system is stated as Fig.3. It consists of primary and secondary control. The RBF-NN sliding-mode secondary controller is proposed in this paper. This controller adjusts the output voltage amplitude $y_i = V_i$ of system (9) by transmitting a control signal $u_i = V_{ni}$ to the primary control to overcome the voltage deviation, re-balances and achieves system stability. The main content of this paper is the secondary control of this framework.

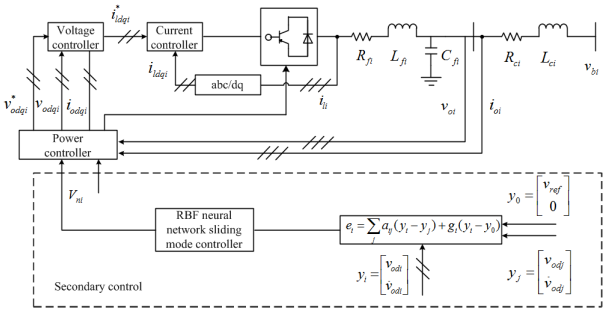

FIGURE 3. The framework of hierarchical control for a MG system.

III. SECONDARY VOLTAGE CONTROLLER

In this paper, the RBF-neural-network (RBF-NN) sliding-mode control algorithm is applied to the distributed secondary control strategy of the MG. RBF-NN sliding-mode control is a control theory that combines the advantages of neural network and sliding variable structure principle. And the detailed knowledge of them can be found in [27] and [28]. The control target is transformed from tracking error to sliding mode function. The input of the controller is not the derivative of error and error but the sliding mode function and its derivative. When the sliding mode function approaches zero, the tracking error will also asymptotically reach zero. Another advantage of RBF-NN sliding-mode control is that the controller does not rely on the accurate mathematical model of the system, and can soften the control signal to reduce the chattering phenomenon caused by general sliding mode control. Therefore, the distributed RBF-NN sliding-mode secondary voltage controller is designed, as shown in Fig.4.

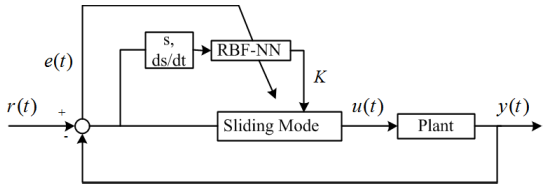

FIGURE 4. RBF-NN sliding-mode secondary voltage controller.

It is assumed that the communication structure graph of the MG is bidirectionally connected, that is, each DG can transmit signals to each other directly connected to. In order to synchronize the voltages of all DGs in MG to their nominal values. The cooperative team objectives are expressed in terms of the local neighborhood tracking error

$$e_i = \sum_{j\in N_i} a_{ij}(y_j - y_i) + b_i(y_r - y_i) \tag{11}$$

where a_{ij} is the elements of the communication digraph adjacency matrix. And $b_i \geq 0$ represents the weight of the communication path between the ith DG and the virtual leader DG. If the reference voltage value (i.e., nominal value) input into the ith DG, then $b_i \neq 0$; N_i represents a set of DGs directly communicating with the ith DG. And the tracking error derivative is

$$e_i^d = \sum_{j\in N_i} a_{ij}(\dot{y}_j - \dot{y}_i) + b_i(0 - \dot{y}_i) \tag{12}$$

We select

$$\begin{cases} z_i = y_r - y_i \\ \dot{z}_i = -\dot{y}_i \end{cases} \tag{13}$$

According to the sliding mode variable structure principle, the corresponding sliding mode function is designed as $s_i = cz_i + \dot{z}_i$, c is positive constant. Thus, the derivative of it is:

$$\begin{aligned} \dot{s}_i &= c\dot{z}_i + \ddot{z}_i \\ &= -c\dot{y}_i - \ddot{y}_i \\ &= -c\dot{y}_i - f_i - \frac{1}{\tau_{Q_i} K_{V_i}} u_i \end{aligned} \tag{14}$$

The control law is derived to from the exponential approach law $\dot{s}_i = -Ksgn(s_i) - \varepsilon s_i$:

$$u_i = -\tau_{Q_i} k_{V_i}[f_i + c\dot{y}_i - Ksgn(s_i) - \varepsilon s_i] \; \varepsilon > 0, \quad K > 0 \tag{15}$$

where ε is constant coefficient of exponential approach, K denotes the rate at which the point of motion of the system approaches the switching plane $s = 0$.

Compared with BP network, RBF network has good generalization capabilities and simple network structure, and avoid unnecessary calculations. The RBF-neural-network can approximate any nonlinear function with arbitrary precision. It is used to approximate the sliding mode switching gain $K(\chi)$. The network algorithm is

$$h_j = exp(\frac{\|\chi - \beta_j\|^2}{2b_j^2}) \tag{16}$$

$$K = W^{*T} h(\chi) + \sigma \tag{17}$$

where χ is the input of the network, j is the jth node of the network hidden layer, $h = [h_j]^T$ is the Gaussian function output of the network, W^* is the ideal weight of the network, σ is the approximation error of the network, and $0 < \sigma \leq \sigma_N$.

The network input is defined as $\chi = [s \quad \dot{s}]^T$, and the network structure is 2-5-1, that is $\beta_j = [\beta_{1j} \quad \beta_{2j}]^T$, b_j, $j = 1, 2, \cdots, 5$, then the network output is

$$\hat{K}(\chi) = \hat{W}^T h(\chi) \tag{18}$$

$$\begin{aligned} K^*(\chi) - \hat{K}(\chi) &= W^{*T} h(\chi) + \sigma - \hat{W}^T h(\chi) \\ &= -\tilde{W}^T h(\chi) + \sigma \end{aligned} \tag{19}$$

where $K^*(\chi) > 0$ is the ideal sliding mode switching gain.

$$\tilde{K}(\chi) = \hat{K}(\chi) - K^*(\chi) \tag{20}$$

Consider the Lyapunov function candidate

$$V = \frac{1}{2}s^2 + \frac{1}{2\gamma}\tilde{K}^2 \tag{21}$$

where $\gamma > 0$.

In order to derive a conditional network adaptive law that satisfies the condition (i.e., $V > 0, \dot{V} \leq 0$).

$$\dot{V} = s\dot{s} + \frac{1}{\gamma}\tilde{K}\dot{\tilde{K}} = s(-f - \frac{1}{\tau_Q K_V}u - c\dot{y}) + \frac{1}{\gamma}\tilde{K}\dot{\tilde{K}} \tag{22}$$

Then, the control law is designed as

$$u = -\tau_Q k_V[f + c\dot{y} - \hat{K}sgn(s) - \varepsilon s] \tag{23}$$

Then, placing (23) into (22) yields

$$\begin{aligned}\dot{V} &= s(-f - \frac{1}{\tau_Q k_V}u - c\dot{y}) + \frac{1}{\gamma}\tilde{K}\dot{\tilde{K}} \\ &= -\hat{K}|s| - \varepsilon s^2 + \frac{1}{\gamma}(\hat{K} - K^*)\dot{\hat{K}}\end{aligned} \tag{24}$$

We take the adaptive law as

$$\dot{\hat{K}}(\chi) = \gamma|s| \tag{25}$$

$$\dot{\hat{K}}(\chi) = \dot{\hat{W}}^T h(\chi) \tag{26}$$

Thus, the adaptive law of RBF-NN sliding-mode control is

$$\dot{\hat{W}}^T = \gamma|s|h^{-1}(\chi) \tag{27}$$

Theorem: The dynamics of the MG system (9) with the distributed secondary voltage controller (23) and the RBF-NN adaptive law (27) is stable and can reduce the deviation of voltage at all DGs caused by primary control.

Proof: Consider the equation (21) as Lyapunov function. We place the RBF-NN sliding-mode control law (23) and the adaptive law (25) into equation (22):

$$\begin{aligned}\dot{V} &= s\dot{s} + \frac{1}{\gamma}\tilde{K}\dot{\tilde{K}} \\ &= s(-f - \frac{1}{\tau_Q k_V}u - c\dot{y}) + \frac{1}{\gamma}(\hat{K} - K^*)\dot{\hat{K}} \\ &= -K^*|s| - \varepsilon s^2\end{aligned} \tag{28}$$

Therefore, $\dot{V} = -K^*|s| - \varepsilon s^2 \leq 0$. When $\dot{V} \equiv 0$, there is $s \equiv 0$. According to the LaSalle invariant set principle, the closed-loop system is asymptotically stable. Thus, if $t \to \infty$, then $s \to \infty$.

Remark: The system is asymptotically stable, indicating that $s \to 0$ means $e \to 0$, the RBF-NN sliding-mode control system is stable, and all DG voltage amplitudes can be restored to the reference value within a limited time.

IV. CASE STUDY

The effectiveness of the designed secondary voltage controller for the islanded MG was verified in the MATLAB/Simulink environment. Take a MG system consisting of four DGs as an example. The MG system structure is shown in Fig.5. The local loads are connected to each DG. Assume that only DG1 can directly obtain the reference voltage, i.e., $b_1 = 1, b_k = 0, k = 2, 3, 4$. Other DGs can interact with neighboring DGs. The network topology is shown in Fig.6.

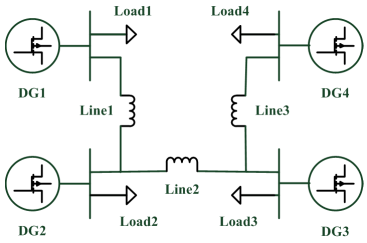

FIGURE 5. MG system structure.

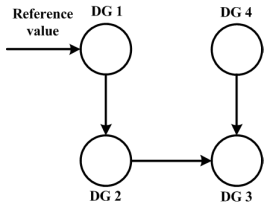

FIGURE 6. Network topology.

The adjacency matrix A corresponding to the topology shown in Fig.6 is

$$A = \begin{bmatrix} 0 & 1 & 0 & 0 \\ 1 & 0 & 1 & 0 \\ 0 & 1 & 0 & 1 \\ 0 & 0 & 1 & 0 \end{bmatrix} \tag{29}$$

The corresponding Laplacian matrix is

$$L = \begin{bmatrix} -1 & -1 & 0 & 0 \\ -1 & 2 & -1 & 0 \\ 0 & -1 & 2 & -1 \\ 0 & 0 & -1 & 1 \end{bmatrix} \tag{30}$$

A. CONTROLLER PERFORMANCE

In this example, the parameters of the simulation system are summarized in Table 1. The simulation is divided into three phases. During $t < 3$s, simulation after the system is disturbed, the MG operates in the islanded mode and the primary control is activated. When $t = 3s$, the secondary control is actived to make the all DG voltages track the reference value $V_r = 380V$. At $t = 5s$, we change the reference voltage of the system to $350V$ to verify the effectiveness of the proposed controller. The simulation results of MG output voltage are shown in Fig.7.

TABLE 1. Parameter values for simulation.

	DG1		DG2		DG3		DG4	
DGs	τ_{Q_1}	0.016	τ_{Q_2}	0.016	τ_{Q_3}	0.016	τ_{Q_4}	0.016
	k_{V_1}	$1e^{-2}$	k_{V_2}	$1e^{-2}$	k_{V_3}	$1e^{-2}$	k_{V_4}	$1e^{-2}$
	k_{Q_1}	$4.2e^{-4}$	k_{Q_2}	$4.2e^{-4}$	k_{Q_3}	$4.2e^{-4}$	k_{Q_4}	$4.2e^{-4}$
Loads	Q_{1_1}	0.01	Q_{1_2}	0.01	Q_{1_3}	0.01	Q_{1_4}	0.01
	Q_{2_1}	1	Q_{2_2}	2	Q_{2_3}	3	Q_{2_4}	4
	Q_{3_1}	$1e^4$	Q_{3_2}	$1e^4$	Q_{3_3}	$1e^4$	Q_{3_4}	$1e^4$
Lines	$B_{12} = 10\Omega^{-1}, B_{23} = 10.67\Omega^{-1}, B_{34} = 10.67\Omega^{-1}$							
Reference	$V_r = 380V$							
Sling-mode	$c_k = 160 \quad k = 1, \cdots, 4$							
	$b_k = 3 \quad k = 1, \cdots, 4$							
RBF-NN	$\beta_k = 0.55 * [-2, -1, 0, 1, 2; \quad -2, -1, 0, 1, 2] \quad k = 1, \cdots, 4$							

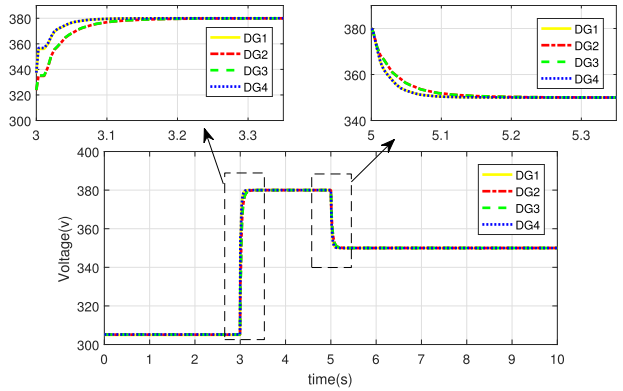

FIGURE 7. Microgrids output voltage.

It can be seen from Fig.7 that during $t < 3$s, the output voltage amplitudes of the MG system keep stable under the primary control. At $t = 3s$, the secondary control starts to work. After about $0.25s$, the system voltage amplitudes track to $380V$ and stabilize, as shown in Fig.7. At $t = 5s$, the reference voltage amplitudes tracked by the system is changed to $350V$. After approximately $0.25s$, the system voltages stabilize again at the reference value, as shown in Fig.7. The result shows that the designed secondary controller starts at $t = 3s$. And it make all output voltage amplitudes in the system recover to the reference value and remain stable.

B. EFFECT OF CONTROLLER PARAMETER C

The RBF-NN sliding-mode secondary controller is employed in this paper. There exists some important parameters influence the effect of this controller. According to sliding mode theory, the error function is defined as $s(t) = cz(t) + \dot{z}(t)$ for tracking problems. Thus, the MG control system performance depends on value c. In the event that other parameters are fixed except c value, we compare the output voltage amplitudes of DG4. We determine the value of c that makes the system response best by analysis. Fig. 8 shows the output voltage response curves with different controller parameters. It can be seen from the figure that the larger the c value, the faster the response. However, when the value exceeds a certain value, the dynamic performance of the system deteriorates. When $c = 50, 110, 150, 160$, the system response speed is gradually increased without overshoot. When $c = 230$, there exits overshoot of the system. When $c = 260$, the output voltage amplitude of system is overshot, which cannot converge at $380V$. Thus, the final control parameter c value is 160. In that case, the RBF-NN sliding-mode controller can make the MG system stable in a short time ($t < 0.25s$). In addition, the chattering phenomenon produced by sliding mode variable structure control is reduced.

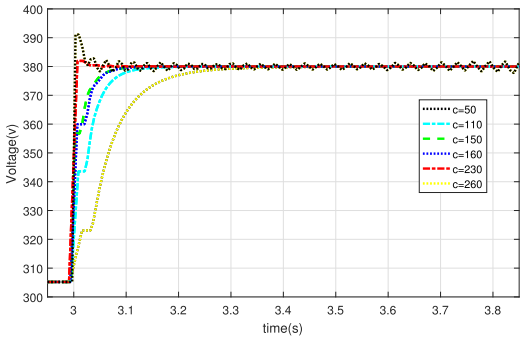

FIGURE 8. Microgrids output voltage with different parameter c.

C. THE OUTPUT OF RBF-NEURAL-NETWORK

Fig. 9 is the output $\hat{K}$ of RBF neural network. It shows four sliding mode gain curve in secondary controllers, using the RBF neural network to approximate the switching gain K of the sliding mode controller. Constantly updating the K value, which is to serialize discontinue the control signal. It is known from the figure that at 5 s, due to the sudden change of the system tracking signal, the RBF network adjusts K value rapidly at this moment to make the system adapt quickly. It illustrates that in the case of disturbances, the control system can be quickly adjusted, with good adaptability.

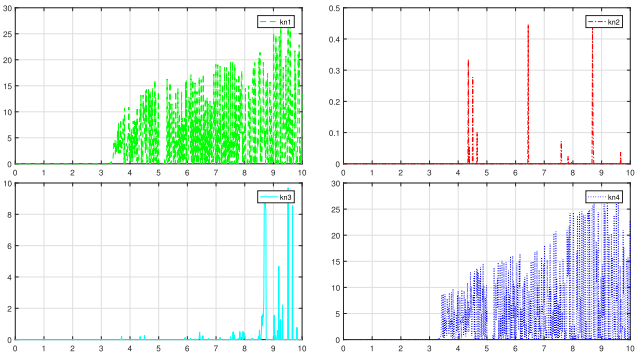

FIGURE 9. RBF neural network output $\hat{K}$.

V. CONCLUSION

In this paper, the secondary control of the MG voltage is designed. For the traditional centralized control structure, the distributed control structure has a simpler communication network and avoids single point of failure. The communication information is transmitted to each other through adjacent DGs, without a centralized control unit. For the design of the secondary controller, the RBF-NN sliding-mode control algorithm is used to solve the voltage restoration problem. Simple sliding mode control may cause chatter, which is weakened by neural network theory. The simulation verifies the effectiveness and adaptability of the algorithm for the secondary voltage control of MG, and the suitable system response speed is achieved by adjusting the controller parameters. In practice, the communication delay and interference in MG system can not be avoided. Therefore, in future studies, we will model the MG system, considering the existence of time delays and noise disturbances in

communication links. And the robust distributed control approach will be discussed and designed for the MG model approximating the actual. We hope that it is meaningful for the control problems of MG.

REFERENCES

[1] X. Yu, C. Cecati, T. Dillon, and M. G. Simões, "The new frontier of smart grids," *IEEE Ind. Electron. Mag.*, vol. 5, no. 3, pp. 49–63, Sep. 2011.
[2] N. M. Dehkordi, N. Sadati, and M. Hamzeh, "Distributed robust finite-time secondary voltage and frequency control of islanded microgrids," *IEEE Trans. Power Syst.*, vol. 32, no. 5, pp. 3648–3659, Sep. 2017.
[3] D. E. Olivares *et al.*, "Trends in microgrid control," *IEEE Trans. Smart Grid*, vol. 5, no. 4, pp. 1905–1919, Jul. 2014.
[4] J. Li, K. Pan, and Q. Su, "Sensor fault detection and estimation for switched power electronics systems based on sliding mode observer," *Appl. Math. Comput.*, vol. 353, pp. 282–294, Jul. 2019.
[5] F. Guo, C. Wen, and Y.-D. Song, *Distributed Control and Optimization Technologies in Smart Grid Systems*, Boca Raton, FL, USA: CRC Press, 2017.
[6] A. Pilloni, A. Pisano, and E. Usai, "Robust finite-time frequency and voltage restoration of inverter-based microgrids via sliding-mode cooperative control," *IEEE Trans. Ind. Informat.*, vol. 65, no. 1, pp. 907–917, Jan. 2018.
[7] N. Pogaku, M. Prodanovic, and T. C. Green, "Modeling, analysis and testing of autonomous operation of an inverter-based microgrid," *IEEE Trans. Power Electron.*, vol. 22, no. 2, pp. 613–625, Mar. 2007.
[8] N. M. Dehkordi, N. Sadati, and M. Hamzeh, "Fully distributed cooperative secondary frequency and voltage control of islanded microgrids," *IEEE Trans. Energy Convers.*, vol. 32, no. 2, pp. 675–685, Jun. 2017.
[9] Q. Shafiee, J. M. Guerrero, and J. C. Vasquez, "Distributed secondary control for islanded microgrids—A novel approach," *IEEE Trans. Power Electron.*, vol. 29, no. 2, pp. 1018–1031, Feb. 2014.
[10] X. Lu, X. Yu, J. Lai, J. M. Guerrero, and H. Zhou, "Distributed secondary voltage and frequency control for islanded microgrids with uncertain communication links," *IEEE Trans. Ind. Informat.*, vol. 13, no. 2, pp. 448–460, Apr. 2017.
[11] J. Lai, X. Lu, X. Yu, and A. Monti, "Cluster-oriented distributed cooperative control for multiple AC microgrids," *IEEE Trans. Ind. Informat.*, to be published. doi: 10.1109/TII.2019.2908666.
[12] M. S. Mahmoud, N. M. Alyazidi, and M. I. Abouheaf, "Adaptive intelligent techniques for microgrid control systems: A survey," *Int. J. Elect. Power Energy Syst.*, vol. 90, pp. 292–305, Sep. 2017.
[13] J. Lai, H. Zhou, X. Lu, X. Yu, and W. Hu, "Droop-based distributed cooperative control for microgrids with time-varying delays," *IEEE Trans. Smart Grid*, vol. 7, no. 4, pp. 1775–1789, Jul. 2016.
[14] J. Schiffer, T. Seel, J. Raisch, and T. Sezi, "Voltage stability and reactive power sharing in inverter-based microgrids with consensus-based distributed voltage control," *IEEE Trans. Control Syst. Technol.*, vol. 24, no. 1, pp. 96–109, Jan. 2016.
[15] J. Lai, X. Lu, X. Yu, W. Yao, J. Wen, and S. Cheng, "Distributed multi-DER cooperative control for master-slave-organized microgrid networks with limited communication bandwidth," *IEEE Trans. Ind. Informat.*, to be published. doi: 10.1109/TII.2018.2876358.
[16] F. Guo, C. Wen, J. Mao, and Y. D. Song, "Distributed secondary voltage and frequency restoration control of droop-controlled inverter-based microgrids," *IEEE Trans. Ind. Electron.*, vol. 62, no. 7, pp. 4355–4364, Jul. 2015.
[17] A. Bidram, A. Davoudi, F. L. Lewis, and J. M. Guerrero, "Distributed cooperative secondary control of microgrids using feedback linearization," *IEEE Trans. Power Syst.*, vol. 28, no. 3, pp. 3462–3470, Aug. 2013.
[18] A. Bidram, A. Davoudi, F. L. Lewis, and Z. Qu, "Secondary control of microgrids based on distributed cooperative control of multi-agent systems," *IET Generat., Transmiss., Distrib.*, vol. 7, no. 8, pp. 822–831, Aug. 2013.
[19] G. Lou, W. Gu, W. Sheng, X. Song, and F. Gao, "Distributed model predictive secondary voltage control of islanded microgrids with feedback linearization," *IEEE Access*, vol. 6, pp. 50169–50178, 2018.
[20] J. Li and D. Zhang, "Backstepping and sliding-mode techniques applied to distributed secondary control of islanded microgrids," *Asian J. Control*, vol. 20, no. 3, pp. 1288–1295, May 2018.
[21] G. Lou, W. Gu, Y. Xu, M. Cheng, and W. Liu, "Distributed MPC-based secondary voltage control scheme for autonomous droop-controlled microgrids," *IEEE Trans. Sustain. Energy*, vol. 8, no. 2, pp. 792–804, Apr. 2017.
[22] J. Schiffer, R. Ortega, A. Astolfi, J. Raisch, and T. Sezi, "Conditions for stability of droop-controlled inverter-based microgrids," *Automatica*, vol. 50, no. 10, pp. 2457–2469, Oct. 2014.
[23] S. Zuo, A. Davoudi, Y. Song, and F. L. Lewis, "Distributed finite-time voltage and frequency restoration in islanded AC microgrids," *IEEE Trans. Ind. Electron.*, vol. 63, no. 10, pp. 5988–5997, Oct. 2016.
[24] R. Bergen, *Power Systems Analysis*. Upper Saddle River, NJ, USA: Prentice-Hall, 1986.
[25] A. Bidram, V. Nasirian, A. Davoudi, and F. L. Lewis, "Droop-free distributed control of AC microgrids," in *Advances in Industrial Control*. 2017, pp. 141–171.
[26] K. Hatipoglu, I. Fidan, and G. Radman, "Investigating effect of voltage changes on static ZIP load model in a microgrid environment," in *Proc. North Amer. Power Symp. (NAPS)*, Sep. 2012, pp. 1–5.
[27] Y. Liu, Q. Zhang, C. Wang, and N. Wang, "A control strategy for microgrid inverters based on adaptive three-order sliding mode and optimized droop controls," *Electr. Power Syst. Res.*, vol. 117, pp. 192–201, Dec. 2014.
[28] Q. Shafiee, Č. Stefanović, T. Dragičević, P. Popovski, J. C. Vasquez, and J. M. Guerrero, "Robust networked control scheme for distributed secondary control of islanded microgrids," *IEEE Trans. Ind. Electron.*, vol. 61, no. 10, pp. 5363–5374, Oct. 2014.

XUEQIANG SHEN received the M.Sc. degree from Northeast Electric Power University, China, in 2008, and the Ph.D. degree from North China Electric Power University, in 2014. From 2015 to 2016, he was a Visiting Scholar with the Intelligent Systems and Biomedical Robotics Group (ISR), University of Portsmouth, U.K. He is currently an Associate Professor with the School of Automation Engineering, Northeast Electric Power University. He has published three articles on SCI journals and five papers on international conferences. His research interests include process control and intelligent control.

HAIQING WANG is currently pursuing the master's degree with Northeast Electric Power University. Her research interest includes power cyber-physical systems.

JIAN LI received the B.Sc. degree in electrical automation and the M.Sc. degree in control theory and application from Liaoning Technical University, China, in 2005 and 2008, respectively, and the Ph.D. degree in control theory and application from Northeastern University, China, in 2013. In 2015, she was a Visiting Scholar with the Nonlinear Dynamics Group, Yeungnam University, South Korea. From 2016 to 2017, she was a Visiting Scholar with the National University of Singapore, Singapore. She is currently an Associate Professor with the School of Automation Engineering, Northeast Electric Power University, China. She has published 22 articles on SCI journals and nine papers on international conferences. Her research interests include fault detection, robust control, and power cyber-physical systems.

QINGYU SU received the B.Sc. degree in electrical automation and the M.Sc. degree in control theory and application from Liaoning Technical University, China, in 2005 and 2008, respectively, and the Ph.D. degree in control theory and application from Northeastern University, China, in 2013. From 2015 to 2016, he was a Visiting Scholar with the Intelligent Systems and Biomedical Robotics Group (ISR), University of Portsmouth, U.K. He is currently an Associate Professor with the School of Automation Engineering, Northeast Electric Power University, China. He has published 21 articles on SCI journals and eight papers on international conferences. His research interests include switched systems, nonlinear control systems, and power cyber-physical systems.

LAN GAO is currently pursuing the master's degree with Northeast Electric Power University. Her research interest includes power cyber-physical systems.